Endosomes facilitate mitochondrial clearance by enhancing Mfn2 degradation and subsequent Parkin recruitment

Rishith Ravindran[1]*, Anoop Kumar G. Velikkakath[1]*, Nikhil Dev Narendradev[1], Aneesh Chandrasekharan[2], T. R. Santhoshkumar[2], Srinivasa M. Srinivasula[1]

[1]School of Biology, Indian Institute of Science Education and Research Thiruvananthapuram, Maruthamala PO, Vithura, Thiruvananthapuram - 695551, Kerala, India.

[2]Cancer Research Program-1, Rajiv Gandhi Centre for Biotechnology, Thiruvananthapuram - 695014, Kerala, India.

*These authors contributed equally to this work.

Correspondence to Srinivasa M. Srinivasula: sms@iisertvm.ac.in

Summary

Mitochondrial quality control and homeostasis is ensured by removal of the damaged mitochondria involving lysosomal and proteasomal degradation mechanisms. Though much remains to be elucidated, recent findings suggest important roles for endosomal machinery in the elimination of damaged mitochondria. In this study, we report a novel function for a FYVE-like domain containing endosomal ubiquitin ligase, CARP2 in mitophagy. Our results show that endosomal CARP2 associates with damaged mitochondria, and this association precedes that of Parkin, whose recruitment is known to be essential for mitochondrial clearance. Association of Parkin to damaged mitochondria was substantially reduced in CARP2 KO cells upon CCCP treatment. We also demonstrate that Mitofusin-2 degradation, which is a prerequisite for Parkin recruitment during damage, was inhibited in CARP2-deficient cells. Hence, we conclude that endosomal-associated CARP2 facilitates mitophagy by regulating Parkin recruitment and activation by targeting Mitofusin-2. Our study proposes a model on how heterogenous endocytic machinery can interact with damaged mitochondria and unravel a new mechanism for mitochondrial clearance.

Introduction

Stringent quality control mechanisms ensure organelle and cellular homeostasis. Signaling pathways that regulate mitochondrial quality and function are believed to play critical roles in diverse physiological processes including cell survival and their dysregulation results in the development of numerous pathological conditions like neurological disorders, cancer and myopathies (Arun, Liu and Donmez, 2015; Ahuja, 2018; Porporato *et al.*, 2018). Autophagy is a conserved intracellular catabolic process in which cytoplasmic contents, including damaged mitochondria, are sequestered in double-membrane autophagosomes and delivered to the lysosomal compartment for degradation (Dikic, 2017). Selective elimination of dysfunctional and damaged mitochondria involving autophagic machinery and lysosomes is known as mitophagy (Montava-Garriga and Ganley, 2020).

Though cells can employ various other cellular tools like ESCRT machinery (Hammerling *et al.*, 2017), MDVs (Mitochondrial Derived Vesicles) (Sugiura *et al.*, 2014; McLelland *et al.*, 2016) etc., to remove mitochondrial contents, mitophagy mediated by PINK1/Parkin is relatively well studied (Narendra *et al.*, 2008, 2010; Durcan and Fon, 2015). In depolarized mitochondria, PINK1 accumulated on the outer mitochondrial membrane phosphorylates Parkin which in turn pleiotropically ubiquitinates Mfn2 resulting in its degradation. Mfn2 degradation mediated by Parkin is believed to be a critical step in Parkin stabilization and mitophagy, as Mfn2 regulates physical attachment of mitochondria to ER. Many details of the sequence of events involved in Parkin recruitment, stabilization and identity of proteins are not available.

Recent reports, however, suggested a role for endosomes and endosomal proteins in mitochondrial clearance. Crosstalk of endosomal related proteins RABGEF1, Rab5, MON1/CCZ1 complex and Rab7A result in Atg9A vesicle recruitment to autophagosome formation site (Yamano *et al.*, 2018). Moreover, Rab5 positive endosomes have been implicated in the elimination of damaged mitochondria via the ESCRT complex machinery, and contribute to cytoprotective roles against oxidative stress (Hammerling *et al.*, 2017; Hsu *et al.*, 2018). It has also been proposed that Rab11A endosomes enable autophagy of damaged mitochondria (Puri *et al.*, 2018). How endosomes influence the

mitochondrial quality and the crosstalk between the endosomal machinery and the above molecules that are known to be critical for mitophagy, remain to be elucidated.

CARP2 (Caspase-8- and -10-associated RING Protein 2) is one of the two RING and FYVE-like domain-containing proteins in the human genome. While the RING domain confers ubiquitin ligase activity, the FYVE-like motif along with its N-terminal sequence is reported to associate with phospholipids like phosphatidylinositol 3-phosphate (McDonald and El-Deiry, 2004). Interestingly, CARP2-positive vesicles are also reported to be positive for Rab5, Rab7, Rab9, Rab11 and Lamp1 markers of diverse endocytic vesicles (Coumailleau *et al.*, 2004; Liao *et al.*, 2008; Okiyoneda *et al.*, 2018). In this study, we report that CARP2-positive vesicles associate with damaged mitochondria. CARP2 targets, in an ubiquitin ligase-dependent manner, Mfn2 for degradation; and contribute to mitochondrial elimination by facilitating Parkin recruitment and stabilization.

Results

Endosomal ubiquitin ligase CARP2 associates with damaged mitochondria

Because the endosomal machinery has been shown to contribute to mitophagy, we investigated the role of CARP2 positive endosomes in mitochondrial elimination. As a first step, we monitored the association between CARP2 endosomes and damaged mitochondria using confocal microscopy of A549 lung carcinoma cells stably expressing CARP2-EGFP. In these cells, mitochondria were stained with MitoTracker Red CMXRos. As expected, in cells treated with DMSO, CARP2-EGFP was primarily localized to intracellular vesicles, which were reported to be positive for various known endosomal markers [Figure 1A, (Okiyoneda *et al.*, 2018)]. In these cells, mitochondria appeared mostly as filamentous structures with minimal association with CARP2 vesicles. However, mitochondria in cells treated with the mitochondrial uncoupler CCCP, were found to be fragmented as expected, with some being surrounded by CARP2 vesicles (Figure 1A). Line scan analysis demonstrated clear encircling of damaged mitochondria by CARP2 (Figure 1B), with nearly 60% of the live cells showing positive-association between these organelles within 25 min of treatment (Figure 1C). Pearson coefficient analysis also showed a positive correlation in CCCP treated cells compared with untreated cells (Figure 1D). Another mitochondrial uncoupler commonly used is valinomycin. Results from cells

treated with valinomycin also showed a similar association that was observed in cells treated with CCCP (Figure S1).

The association of CARP2 vesicles with damaged mitochondria was further analyzed by super-resolution imaging [Structured Illumination Microscopy (SIM)] in cells stably expressing EBFP2-Mito-7 and CARP2-mRFP (Figure 1E). The encirclement of damaged mitochondria by CARP2 positive vesicles was also noted in 3D super-resolution SIM images (Figure 1F and Movie1).

We examined the dynamics of association between endosomes and damaged mitochondria. Time-lapse live imaging analysis of cells stably expressing CARP2-EGFP and stained with MitoTracker Red CMXRos, over a period of 12 min revealed formation of protrusions of GFP positive structures from CARP2 vesicles towards damaged mitochondria (Figure 2A, Movie 2), which transiently hover around mitochondria. To further understand this process we have used photobleaching strategy. A549 cells stably expressing CARP2-EGFP were exposed to bleaching using 488nm Argon laser at a region of Interest, consisting of CARP2-positive mitochondria. Immediately after bleaching, the movement of CARP2 vesicles (green) in the vicinity of damaged mitochondria (red) was monitored for a period of 2 min. As early as 41 seconds after photobleaching, movement of GFP-positive structures from the surrounding area of the bleached region towards the damaged mitochondria was noted (Figure 2B, Movie 3). As pointed by arrows these structures appeared tubular in nature, as long as 3μm. Moreover, under these conditions the mitochondria were surrounded with multiple CARP2-positive vesicles within two minutes, suggesting a critical role for CARP2 positive endosomes in mitochondrial homeostasis, probably by contributing to the elimination of damaged mitochondria.

FYVE-like motif, predicted palmitoylation sites (C5, 6) and ubiquitin ligase domains are the functional domains of CARP2 (Figure 2C). To understand the role of these domains on the association of CARP2 with damaged mitochondria, we have generated CARP2 KO A549 cells using CRISPR-Cas9 system and these cells were reconstituted with EGFP tagged CARP2 variants. These reconstituted cells were stained with MitoTracker Red CMXRos and the effect of various CARP2 mutations on their localization to damaged mitochondria were assessed (Figure 2D). The expression of WT or deletion FYVE-like or

ligase mutant (H333A) or C5, 6A mutants from untreated cells is shown by western blotting (Figure 2E). In contrast to other FYVE domain-containing proteins, deletion of FYVE-like domain of CARP2 still appeared as punctate structures. This could be because in addition to FYVE-like domain, there are N-terminal cysteine residues predicted to be palmitoylated and may be important for membrane localization (Araki *et al.*, 2003; Okiyoneda *et al.*, 2018). Interestingly, unlike WT CARP2 which showed ring-like pattern around damaged mitochondria, ubiquitin ligase mutant (H333A) showed no ring formation with intracellular vesicles and rather appeared as weak CARP2-EGFP signals showing colocalization with damaged mitochondria. However, neither ring formation nor colocalization was observed between damaged mitochondria with localization defective CARP2 variant C5, 6A. Association of deletion FYVE-like mutant with damaged mitochondria were also monitored and was found to be significantly less compared to WT CARP2. Quantitative association of all these variants with MitoTracker are shown (Figure 2E).

CARP2 promotes a reduction in mitochondrial protein levels in a ubiquitin ligase activity-dependent manner

To assess the functional consequence of CARP2 association with damaged mitochondria in terms of reduction of mitochondrial specific proteins, cells stably expressing CARP2 without tag or mRFP tagged were generated in A549 and U2OS, respectively. To measure mitochondrial clearance, we monitored levels of two mitochondrial proteins, TIMM23, an inner mitochondrial membrane (IMM) protein, and Complex III core I (COMIII), IMM/matrix protein (Yoshii *et al.*, 2011; Klionsky *et al.*, 2016) in CARP2 stably expressing cells with or without CCCP treatment.

Consistent with the association of CARP2 with damaged mitochondria, a notable reduction in both COMIII and TIMM23 protein levels were observed in CARP2 stably expressing cells compared to control cells upon CCCP treatment (Figure 3A). Quantification of the intensity of the bands relative to tubulin showed a significant reduction of both proteins, suggesting that CARP2 contributes to the elimination of damaged mitochondria (Figure 3B). To investigate whether CARP2-mediated reduction in mitochondrial protein levels require its ubiquitin ligase activity, we have compared

reduction in the levels of both these proteins in A549 cells stably expressing either CARP2 WT or H333A mutant (ubiquitin ligase inactive mutant). The reduction in the levels of COMIII and TIMM23 was comparatively less in H333A variant than WT CARP2 stably expressing cells, indicating the requirement of ubiquitin ligase activity in the elimination of mitochondrial proteins (Figure S2A).

To understand the functions of CARP2 vs. Parkin in mitophagy, we monitored the levels of COMIII in U2OS cells stably expressing CARP2-mRFP or mRFP alone along with YFP-Parkin. At 6 h of CCCP treatment, CARP2-mRFP stably expressing cells showed an enhanced reduction of damaged mitochondria represented by COMIII when compared to mRFP only controls (Figure 3C), suggesting of an interactive relationship between these proteins. Similar results with TIMM23 were noticed in A549 cells stably expressing CARP2 without tag and YFP-Parkin (Figure S2B). These results collectively indicate the cross-talk between endosomal ubiquitin ligase CARP2 and cytosolic ubiquitin ligase Parkin in the clearance of damaged mitochondria.

CARP2 associates with damaged mitochondria before Parkin

To understand this cross-talk in detail we monitored the localization of CARP2 and Parkin in CCCP treated A549 cells, stably expressing CARP2-EGFP or YFP-Parkin individually and pre-stained with MitoTracker Red CMXRos. As shown (Figure 4A), in these cells CARP2 localization to mitochondria was observed within 10 minutes of treatment, whereas that of Parkin was noted only after 30 minutes (Figure 4 B) indicating that CARP2 localization precedes that of Parkin and the association of CARP2 is probably required for Parkin localization. To investigate whether the kinetics of recruitment of both these proteins to mitochondria is specific to A549 cells, or similar pattern can be observed in other cells, we stably expressed both CARP2-mRFP and YFP-Parkin simultaneously in U2OS cell line. Simultaneous expression of these proteins also helped to monitor their relative recruitment vs. mitochondria. As seen in A549 cells, CARP2 recruitment to mitochondria was found in early time points compared to Parkin recruitment. Surprisingly, very little co-localization between mitochondria that associates with CARP2 and Parkin was noted (Figure 4C). Time-course measurements indicated maximum localization of CARP2 within 10 min whereas Parkin peaked after 30min (Figure 4D). However, close

proximity between CARP2- and Parkin-positive mitochondria was observed, without overt localization. These results suggest that CARP2 either localizes transiently at early time points or localizes to a different set of mitochondria population or both. A significant difference in the ratio of Parkin's modified (probably ubiquitinated) and unmodified levels that was noted in CARP2 stably expressing cells compared to mRFP alone control (Figure 3C, D) suggests that apparently distinct populations are somehow connected and influence each other. This raises the possibility that CARP2 might contribute to mitophagy by affecting the modification of Parkin. Thus we hypothesized that CCCP treated CARP2 KO cells should have lesser Parkin modification and reduced localization to the mitochondria.

CARP2 is required for the stable recruitment of Parkin on damaged mitochondria and modulating mitophagy

To investigate such an idea, first we measured the status of Parkin localization to damaged mitochondria in CARP2 KO cells stably expressing YFP-Parkin. In DMSO treated cells, YFP-Parkin remained cytosolic in both Wild-Type (WT) and CARP2 KO. In WT cells upon CCCP treatment, YFP-Parkin appeared as punctate structures, indicating its localization to damaged mitochondria. However, in CARP2 KO, very little relocation of YFP-Parkin to mitochondria was observed, with most of the cells showing cytoplasmic Parkin. These differences are more pronounced in 6 h after treatment than 2 h (Figure 5A). These results indicate that CARP2 is required for the stable recruitment of Parkin to mitochondria. Quantification of these observations are shown (Figure 5B). Because mitochondrial association of Parkin is required for the removal of this organelle, we measured the levels of COMIII and TIMM23 in CARP2 KO or ATG5 KO background. The levels of both these proteins were much higher in CARP2 KO cells than in WT control cells, suggesting that the inability of Parkin to localize to mitochondria affected their elimination (Figure 5C, D). In ATG5 KO cells also similar levels of these proteins were observed. These results collectively demonstrate that CARP2 function is essential for Parkin recruitment to the damaged mitochondria and its subsequent elimination.

CARP2 contributes to ubiquitination and degradation of Mitofusin-2

Our investigations into the molecular mechanisms on how CARP2 regulates Parkin recruitment, led us to Mfn2 (Mitofusin-2). Mfn2 is a 757 amino acid GTPase that facilitates fusion of mitochondria and tethering of mitochondria with ER (Santel and Fuller, 2001; De Brito and Scorrano, 2008). A recent study suggested that the degradation of Mfn2 is critical for Parkin recruitment to damaged mitochondria (McLelland *et al.*, 2018). Since deficiency of CARP2 also showed a decrease in the association of Parkin with damaged mitochondria, we hypothesized that CARP2 might be functioning by targeting Mfn2. To investigate this further, we have followed Mfn2 levels in CCCP treated A549 cells, cells which are reported to express very little endogenous Parkin (Villa *et al.*, 2017). Upon CCCP treatment, reduced endogenous Mfn2 levels were noted in CARP2 stably expressing cells and this reduction requires CARP2 ubiquitin ligase activity (Figure 6A). The similar or better reduction was observed in the levels of transiently expressed Mfn2-YFP, in a stimulation dependent manner, when this cDNA was expressed in 293T cells along with WT CARP2. These results supported the idea that Mfn2 could be targeted for degradation by CARP2. As hypothesized, treatment of cells with Bafilomycin A1 and MG132 results in recovery of Mfn2-YFP even in the presence of transiently expressed WT CARP2 (Figure 6B). Since a recent study reported of Parkin-mediated phosphoubiquitin burst on Mfn2 within 1 h of CCCP treatment (McLelland *et al.*, 2018) and as we found that Parkin recruitment is adversely affected in the absence of CARP2, we investigated the status of Mfn2 in the absence of CARP2 in A549 cells stably expressing YFP-Parkin. Consistent with less Parkin recruitment shown in Figure 5A, a reduction in modified bands of Mfn2 (previously characterized as Mfn2 phosphoubiquitin burst by McLelland *et al.*, 2018) was noted within 1hr of CCCP treatment in CARP2 KO cells compared to WT A549 cells (Figure 6C and 6D). Moreover, the level of Mfn2 after 4 h treatment remained high in CARP2 KO than in WT cells indicating that CARP2 contributes to ubiquitin burst on Mfn2 and its subsequent degradation upon CCCP treatment (Figure 6 C). These data collectively indicate that CARP2 plays a critical role in mitophagy by mediating modification of Mfn2 and subsequent Parkin recruitment.

Discussion

Endosomes or endosomal-associated Rab family of proteins have recently been reported to play crucial roles in maintaining mitochondrial quality and in the clearance of damaged mitochondria. Whereas one report revealed mitochondrial elimination via ESCRT machinery involving Parkin-dependent sequestration of these organelles into Rab5-positive endosomes (Hammerling *et al.*, 2017), another report strongly suggested the involvement of endosomal Rab cycles in the regulation of mitophagy (Yamano *et al.*, 2018). Reports also suggested that Rab proteins not only facilitates the assembly of autophagosomes downstream of Parkin assembly on damaged mitochondria but also protect mitochondria against oxidative stress (Hsu *et al.*, 2018). Endosome-mitophagy field is still in its infancy with most of the molecular details of the functional cross-talk between the endocytic system and mitochondria waiting to be unravelled. In this report, we provide evidence for a novel mechanism (Figure 6E), that explains the endosomal regulation of mitophagy. Our investigations showed that an endosomal associated ubiquitin ligase CARP2 targets Mfn2, an ER-mitochondria tethering protein, whose degradation is a prerequisite for stable recruitment of Parkin onto damaged mitochondria (McLelland *et al.*, 2018). We demonstrated enhanced degradation of endogenous Mfn2 in CCCP-treated CARP2 expressing cells. Consistent with the idea that Mfn2 can be a target for CARP2, in YFP-Parkin stable cells, deletion of CARP2 not only stabilized Mfn2, but substantially reduced Parkin recruitment to damaged mitochondria. Moreover, the absence of CARP2 also affected CCCP-mediated modified Parkin level, which is reported to be a critical step for mitophagy (Figure 6C). From these results, we conclude that CARP2 modulates Parkin recruitment to damaged mitochondria by targeting Mfn2. Given the reports that ER-mitochondria contact via Mitofusin-2 precludes Parkin recruitment to mitochondria, it would be interesting to study this association in CARP2 KO cells.

Our evidence suggests that CARP2 associated endosomes somehow sense mitochondrial damage and associate with them. CARP2 protein contains a FYVE-like domain which unlike other FYVE proteins does not have a membrane anchoring motif (Tibbetts *et al.*, 2004). However, with the post-translational modifications like palmitoylation, it helps the molecule to anchor to the membrane (Araki *et al.*, 2003). In agreement with this theory, we and others found that amino acid cysteine at 5th and 6th positions (predicted to be palmitoylation site) are required for endosomal association

[Figure 2D and (Okiyoneda *et al.*, 2018)]. Interestingly, a variant without FYVE-like domain (39-92 aa) though localizes to endosomes, it is still unable to associate with damaged mitochondria. These results suggest that FYVE-like domain of CARP2 might be required for the trafficking of vesicles as it has been reported in several other FYVE domain-containing proteins like Vac1, EEA1 etc. (Stefan, Audhya and Emr, 2010). Moreover, a variant (C5, 6A) that is unable to associate with endosomes also did not localize to damaged mitochondria. These results imply that it is the vesicles, not the CARP2 protein, themselves are in contact with damaged mitochondria.

Time-lapse imaging identifies damaged mitochondria into two populations of CARP2-positive and Parkin-positive. Association of CARP2 was observed as early as 10 min whereas that of Parkin takes at least 30min. Knockout of CARP2 reduces both Parkin modification and its recruitment to damaged mitochondria; we believe that these two populations are linked and reflect different hierarchical stages, with CARP2 facilitating Parkin recruitment by targeting Mfn2 as discussed above. One of the mitochondrial ubiquitin ligases, MARCH5/MITOL has recently been shown to ubiquitinate mitochondrial protein(s) constitutively and this modification appears to contribute to Parkin recruitment (Koyano *et al.*, 2019). MITOL knockout cells have reduced Parkin recruitment in the early stage of CCCP treatment, beyond 90 min showing similar levels of recruitment. Unlike MITOL, CARP2 is localized to endosomes and lack of CARP2 affected Parkin recruitment even as late as 6 h of CCCP treatment. Hence we conclude that CARP2 plays a major role in mitophagy and in our knowledge this is the first report of any endosomal protein modulating Parkin recruitment. However, this does not limit the ability of CARP2 endosomes in regulating canonical mitophagy, rather opens up the plausible role of these endosomes in other mitochondrial clearance pathways like Parkin independent mitophagy and MDV mediated mitochondrial clearance.

Acknowledgements

We wish to thank DST-INSPIRE for the fellowship of RR, DBT for the fellowship of AKV and IISER TVM for the fellowship of NDN. This project is partly funded by Department of Biotechnology support for lifetime imaging facility awarded to TRS, Department of Biotechnology grant (BT/PR21325/BRB/10/1554/2016), Department of Science and

Technology-Science and Engineering Research Board (DST-SERB) grant (EMR/2016/008048) and IISER TVM intramural funding awarded to SMS. We also thank Nayan Suryawanshi for technical help, Anurup KG for super-resolution microscopy imaging support and Prof. M.K Mathew for helpful discussion during manuscript preparation.

Author contributions

RR, AKV, NDN and AC performed the experiments and acquired the data. RR, AKV, NDN, SMS and TRS critically analyzed the data. RR, AKV, NDN and SMS wrote the manuscript. RR, AKV, NDN and SMS conceived the project and planned the experiments.

Declaration of interest

The authors declare that they have no conflict of interest.

Figure legends

Figure 1. Endosomal CARP2 ubiquitin ligase associates with damaged mitochondria (**A**) A549 cells stably expressing CARP2-EGFP stained with MitoTracker Red CMXRos for 30 min were treated with DMSO or 20μM CCCP. Images of live cells were taken during 10-25 min of CCCP treatment. Scale 2μm, inset scale 1μm. (**B**) Line scan analysis of the area under the arrow are shown. Association of CARP2-EGFP with MitoTracker in cells is quantified using manual counting (**C**) and Pearson correlation coefficient (**D**). Error bars represent mean ± SEM in case of **C** and mean ± SD in case of **D**. All results are from three independent experiments and a minimum of 50 cells were included per experiment. Statistical significance was calculated using two-tailed unpaired t-test. $p = 0.0004$ for C and $p = 0.0005$ for D. (**E**) U2OS cell line stably expressing EBFP2-Mito-7 and CARP2-mRFP along with YFP-Parkin (not shown) were treated with 20μM CCCP and images of live cells were captured using super-resolution microscopy at 14 h post-treatment. Scale 2μm, inset scale 1μm. (**F**) Super-resolution 3D still images in four different angles of EBFP2-Mito-7-positive mitochondria and CARP2-mRFP-positive endosomes shown as a movie (Movie 1). Scale 1.8μm.

Figure 2. Association of CARP2 with damaged mitochondria requires its FYVE-like domain and predicted palmitoylation sites

(**A**) Time-lapse images of A549 stably expressing CARP2-EGFP live cells stained with MitoTracker Red CMXRos are shown after 14 h of CCCP (20μM) treatment (chosen frames). White arrows indicate CARP2-EGFP-positve vesicles in proximity with MitoTracker Red CMXRos at the indicated time points, scale 2μm and inset scale 1μm. These results are also presented as a movie (Movie 2) shown at 6 frames/s. (**B**) After 18 h of CCCP treatment, cells with CARP2-EGFP around MitoTracker Deep Red FM, were imaged live before and after photobleaching (chosen frames are shown). Circles show the region of photobleaching. Arrows show the movement of CARP2-EGFP-positive vesicles towards the photobleached region. The contrast of the MitoTracker panel alone is adjusted in frames after photobleaching for better visibility. CARP2-EGFP settings are kept the same before and after photobleaching. Scale 1μm. The same results are presented as a movie (Movie 3) shown at 6 frames/s. Frames from 10 s to 20 s of the movie shows zoomed ROI during photobleaching, which is a software automated image processing. (**C**) Schematic representation of CARP2 with domains, predicted palmitoylation sites (* cysteines at 5th and 6th positions) and conserved histidine residue (*H at 333rd position). (**D**) A549 CARP2 KO cells reconstituted with indicated EGFP tagged CARP2 variants, pre-stained with MitoTracker Red CMXRos were treated with 20μM CCCP. Representative images of live cells over 10-40 min of treatment are shown. Scale 2μm, inset scale 1μm. (**E**) Bar graph showing the percentage of cells with more than four CARP2-EGFP puncta localized to MitoTracker during this period. Error bars represent mean ± SEM from three independent experiments. Minimum of 50 cells were counted per experiment. Statistical significance was determined using ordinary one-way ANOVA followed by Tukey's multiple comparisons test. P-values for WT CARP2 (C2) vs. ΔFYVE C2 is 0.0023, WT C2 vs. H333A C2 is 0.0665 and for WT C2 vs. C5, 6A C2 is <0.0001. Western blot showing the expression of WT and mutant variants of CARP2-EGFP are shown in the lower panel.

Figure 3. CARP2 promotes the reduction of damaged mitochondrial proteins in a ubiquitin ligase activity dependent manner (**A**) Western blot showing levels of

indicated proteins in A549 cells stably expressing either EV (Empty Vector) or CARP2 untagged, 24 h after DMSO or 20μM CCCP treatment. * denotes non-specific band. (**B**) The bar graph shows normalized band intensity of COMIII or TIMM23 to Tubulin. Normalized DMSO values were set to 1. Error bars represent mean ± SD from three independent experiments. Statistical significance was calculated using two-tailed unpaired t-test. p = 0.025 for TIMM23 and p = 0.0184 for COMIII. (**C**) Western blot showing levels of the indicated proteins in U2OS cells stably expressing YFP-Parkin along with EBFP2-Mito-7 and either mRFP or CARP2-mRFP cells at indicated time point treated with either DMSO or 20μM CCCP. (**D**) The bar graph shows the band intensity of modified/unmodified form of Parkin. Error bars represents mean ± SD from three independent experiments. Statistical significance was calculated using ordinary two-way ANOVA followed by Tukey's multiple comparisons test. p = 0.0221 for mRFP at 6 h CCCP vs. CARP2-mRFP at 6 h CCCP, p = 0.0018 for mRFP at 9 h CCCP vs. CARP2-mRFP at 9 h CCCP.

Figure 4. CARP2 associates with damaged mitochondria before Parkin A549 cells stably expressing CARP2-EGFP (**A**) or YFP-Parkin (**B**) stained with MitoTracker Red CMXRos for 30 min and treated with 20μM CCCP. Images of live cells at the indicated time points after treatment are shown. (**C**) U2OS cell line stably expressing CARP2-mRFP and YFP-Parkin pre-stained with MitoTracker Deep Red FM for 30 min followed by 20μM CCCP treatment. Images of live cells at the indicated time points after treatment are shown. YFP-Parkin-Mitotracker shown with arrows and CARP2-mRFP-Mitotracker population shown with arrowheads. (**D**) Graph represents cells showing association of mitochondria with CARP2-EGFP or YFP-Parkin at indicated time points. Data is from three independent experiments and a minimum of 50 cells were counted per experiment. Error bars show mean ± SEM.

Figure 5. CARP2 is required for the stable recruitment of Parkin on damaged mitochondria and modulating mitophagy (**A**) A549 Wild Type (WT) or A549 CARP2 KO cells stably expressing YFP-Parkin (Green) were imaged live at the indicated time points after treating with DMSO or 10μM CCCP. Scale 5μm. (**B**) The number of YFP-

Parkin puncta per cell and total YFP-Parkin pixel area per cell were calculated using ImageJ software, each with at least 50 cells per experiment and the graph was plotted. Error bar represent mean ± SEM from three independent experiments. Statistical significance was calculated using two-tailed unpaired t-test. For 2 h (1.5 – 2.5 h) CCCP treatment, p = 0.1560 (total Parkin puncta/cell) and p = 0.0929 (total Parkin pixel area/cell). For 6 h (6 - 7 h) CCCP treatment, p = 0.0048 (total Parkin puncta/cell) and p = 0.0044 (total Parkin pixel area/cell). (**C**) Western blot showing levels of the indicated proteins in A549 cells (WT or ATG5 KO or CARP2 KO) stably expressing YFP-Parkin treated with DMSO or 20μM of CCCP for 24 h. * denotes nonspecific band. (**D**) The bar graph shows band intensity of COMIII or TIMM23 normalized to Tubulin. Error bars represent mean ± SD from three independent experiments. Statistical significance was calculated using two-tailed unpaired t-test. p = 0.0074 for COMIII and p = 0.0008 for TIMM23.

Figure 6. CARP2 modulates Mfn2 modification and degradation

(**A**) Western blot showing levels of endogenous Mfn2 in the lysate of A549 cells expressing EV or CARP2 variants treated with DMSO or 20μM CCCP for 45min. (**B**) 293T cells were transiently transfected with Mfn2-YFP along with either EV or WT CARP2 untagged. Levels of Mfn2-YFP were assessed with anti-GFP antibody after 2 h treatment with DMSO or 20μM CCCP or 20μM CCCP in the presence of MG132 (25μM) and Bafilomycin A1 (200nM). (**C**) Cell lysates of A549 (WT or CARP2 KO) stably expressing YFP-Parkin were assessed for the indicated proteins using western blotting. Red line indicate modified Mfn2 bands. (**D**) Bar graph shows ratio of the modified/unmodified bands of endogenous Mfn2 of **C**. DMSO values were set to 1. Error bars represent mean ± SD from three independent experiments. Statistical significance was calculated using an ordinary two-way ANOVA followed by Tukey's multiple comparisons test, p = 0.0056 and ns = 0.4296. (**E**) Model of CARP2-positive endosome mediated regulation of mitophagy: When mitochondria are healthy, Parkin is cytosolic and CARP2 positive endosome association with mitochondria is minimal. After mitochondrial damage, CARP2 localized to fragmenting mitochondria before Parkin. This is followed by the degradation of Mfn2 by CARP2. Mfn2 degradation promotes stable recruitment of Parkin on damaged mitochondria.

Materials and methods

Cell culture and generation of stable cell lines

All cells were maintained in Dulbecco's modified Eagle's medium (DMEM plus Glutamax Gibco Cat#: 10569-010) containing 10% heat-inactivated FBS (Gibco Cat#: 10270-106) and 1% penicillin-streptomycin (HiMedia Cat#: A001A) in a 5% CO2 incubator at 37°C. For inducing mitochondrial damage, 80-85% confluent cells were treated with Carbonyl cyanide-m-chlorophenylhydrazone (CCCP) (Sigma, Cat#: C-2759) or Valinomycin (Sigma, Cat#: V0627) after 18hrs of plating. For the inhibition of proteasomal and lysosomal degradation, MG132 (Sigma, Cat#: M7449) and Bafilomycin A1 (ChemCruz, Cat#: sc-201550) was used respectively. Mitochondria was stained with 100nM of either MitoTracker Red CMXRos (Invitrogen, Cat#: M7512) or MitoTracker Deep Red FM (Invitrogen, Cat#: M22426) for 30min in culture media followed by one wash in DMEM before CCCP treatment. To develop U2OS cells stably expressing YFP Parkin and EBFP2-Mito-7, initially, the cells were transfected with YFP Parkin and stable cells were generated by selection using G418 (Sigma, Cat#: A1720). The stably expressing cells were further transfected with EBFP2-Mito-7 and cells expressing both the transgene were sorted using flow cytometer sorter equipped with 375-nm laser for EBFP excitation (FACS Aria III). Multiple clones were expanded after further selection in G418 for two weeks and stably expressing clones were used for the current study. Cells stably expressing CARP2-EGFP were generated as per previous protocol (Kitamura *et al.*, 2003). Briefly, HEK293T cells were transfected with pMYsIP-CARP2-EGFP along with pCAG-VSVG and pUMVC plasmids using Lipofectamine 3000 reagent (Invitrogen Cat#: L3000-015). Four days post-transfection, cell supernatants were harvested and were incubated with A549 or U2OS cells in the presence of 4µg/mL Polybrene (Sigma, Cat#: H9268). Cells were cultured in Puromycin (1µg/mL) (Sigma Cat#: P8833) containing DMEM for selection. Other stable cell lines mentioned were also prepared using a similar protocol.

Plasmids, Antibodies and Reagents

Human CARP2 cDNA (NCBI reference sequence: NM_001017368.2:141-1232) and its variants were cloned to pMYs-IP (Kitamura *et al.*, 2003). Mfn2-YFP was a generous gift

from Atsushi Tanaka (Tanaka *et al.*, 2010). Following constructs used were received from Addgene, YFP-Parkin was a gift from Richard Youle (Addgene plasmid#: 23955) (Narendra *et al.*, 2008), EBFP2-Mito-7 was a gift from Michael Davidson (Addgene plasmid#: 55248) (Shaner, Patterson and Davidson, 2007), pCAG-VSVG was a gift from Arthur Nienhuis and Patrick Salmon (Addgene plasmid#: 35616), pUMVC was a gift from Bob Weinberg (Addgene plasmid#: 8449) (Stewart *et al.*, 2003), PX458 was a gift from Feng Zhang (Addgene plasmid#: 48138) (Ran *et al.*, 2013). Following antibodies were used in this study, RFP antibody (Chromotek Cat#: 5f8-100), Polyclonal CARP2 antibody raised in Rabbit (Generated in our laboratory), GAPDH (Abgenex Cat#: 10-10011), Tubulin (Sigma-Aldrich Cat#: T6199), ATG5 (CST Cat#: 12994T), UQCRC1 (For Complex III, Core I, Invitrogen Cat#: 16D10AD9AH5), TIMM23 (SCBT Cat#: sc-514463), GFP (Mouse Living Colours Clonetek Cat#: 632375), Parkin (SCBT Cat#: sc-32282), Mfn2 (Proteintech Cat#: 12186-1-AP) Anti-mouse HRP (Invitrogen Cat#: 61-6520), Anti-rabbit HRP (Invitrogen Cat#: 65-6120), Anti-rat HRP (Jackson ImmunoResearch Cat#: 712-035-150).

Western Blotting

18 h after plating, cells at 80-85% confluency were washed and pelleted at 850×g in ice cold PBS. Cell lysis was done in ice for 30 min using lysis buffer containing 50mM Tris-Cl pH 7.5, 1mM EDTA pH 8, 150mM Sodium chloride, 1% TritonX-100, 1mM Phenylmethylsulfonyl fluoride (PMSF Cat# P7626) and 1X Protease inhibitor cocktail (Sigma Cat# P8340). Supernatant was collected after centrifuging the lysate at 13500×g for 10 min at 4°C. Total protein levels in the supernatant was normalized using BCA (Pierce BCA Protein Assay Kit Cat#: 23225). Samples were mixed with Laemmli buffer and heated for 10min at 95°C before loading them into SDS-PAGE. Samples used to detect modified bands of Mfn2, were processed differently by heating at 37°C for 10 min. Samples separated in SDS-PAGE were later transferred to PVDF membrane (Merck Cat#: IPVH00010). Immunoblot analysis was performed by using antibodies as indicated. They were visualized with chemiluminescent HRP substrate (Merck Cat#: WBKLS0500). Signal intensities were calculated using Quantity One version 4.6.9.

CRISPR KO preparation

A549 cells were transfected with PX458 containing CARP2 or ATG5 gRNAs using Lipofectamine 3000 and sorted for GFP positive cells after 3 days of transfection using flow cytometry. Later, cells were serially diluted and plated in 96 wells to grow single colonies. Knockout of CARP2 or ATG5 from each clone were confirmed using western blot. Sequence of gRNA used are as follows: CARP2 5'-GGTGGAACCATGCTGGAGTG-3' and ATG5 5'-AACTTGTTTCACGCTATATC- 3'.

Live cell imaging

Live cell imaging was performed after 18 h of plating of cells in glass bottom dishes (MatTek 254 Corporation, Cat#: P35G-1.0-20-C). Glass bottom dishes were placed into an on-stage incubator with 5% CO_2 and 37°C. Images were acquired using Leica TCS SP5 II laser scanning confocal microscope with a 63X or 100X 1.4 NA oil-immersion objective lens. Photo bleaching was carried out using a 488nm argon laser at 80% laser power on a chosen ROI (Region Of Interest). Representative confocal images used for figure preparation were noise reduced using LAS AF median filtering, keeping the same settings for all samples. Unprocessed images were used for all quantifications, except for line scan analysis. Super-resolution imaging was carried out using Structured Illumination Microscopy (3D-SIM), N-SIM from Nikon (Tokyo, Japan). Cells grown in glass bottom dishes were maintained at 5% CO2 with 37°C using an on-stage incubator from Tokai Hit (Japan). Cells were imaged using 100 x 1.49 NA oil immersion objective. Images taken using EMCCD Camera iXon 897 (Andor, USA) were reconstructed using NIS elements software following standard protocol.

Statistical analysis

Data were collected from at least three independent experiments and are shown as mean ± SEM or mean ± SD as indicated. Significance levels were set at $\propto = 0.05$. *$P < 0.05$, **$P < 0.01$, and ***$P < 0.001$. All statistical analyses were performed in GraphPad Prism (Version 8.3.1).

Supplemental figures

Supplemental figure S1. **CARP2-positive endosomes localize on mitochondria after valinomycin treatment**

A549 cells stably expressing CARP2-EGFP pre-stained with MitoTracker Red CMXRos was treated for 20μM valinomycin and images were acquired after 3.5 h post-treatment. Scale 2μm, inset scale 1μm.

Supplemental figure S2. **CARP2 is involved in the reduction of mitochondrial proteins after CCCP treatment**

(**A**) Western blot showing levels of indicated proteins in A549 cells stably expressing either EV or CARP2 untagged WT or CARP2 H333A untagged, 24 h after treating with DMSO or 20μM CCCP. (**B**) A549 stably expressing YFP-Parkin in EV or CARP2 untagged were treated with DMSO or 20μM of CCCP for indicated time points and subjected to western blot.

References

Ahuja, A. S. (2018) 'Understanding mitochondrial myopathies: A review', *PeerJ*, 2018(5). doi: 10.7717/peerj.4790.

Araki, K. *et al.* (2003) 'A palmitoylated RING finger ubiquitin ligase and its homologue in the brain membranes', *Journal of Neurochemistry*, 86(3), pp. 749–762. doi: 10.1046/j.1471-4159.2003.01875.x.

Arun, S., Liu, L. and Donmez, G. (2015) 'Mitochondrial Biology and Neurological Diseases', *Current Neuropharmacology*, 14(2), pp. 143–154. doi: 10.2174/1570159x13666150703154541.

De Brito, O. M. and Scorrano, L. (2008) 'Mitofusin 2 tethers endoplasmic reticulum to mitochondria', *Nature*, 456(7222), pp. 605–610. doi: 10.1038/nature07534.

Coumailleau, F. *et al.* (2004) 'Over-Expression of Rififylin, a New RING Finger and FYVE-like Domain-containing Protein, Inhibits Recycling from the Endocytic Recycling Compartment', *Molecular Biology of the Cell*, 15(10), pp. 4444–4456. doi: 10.1091/mbc.e04-04-0274.

Dikic, I. (2017) 'Proteasomal and Autophagic Degradation Systems', *Annual Review of Biochemistry*, 86(1), pp. 193–224. doi: 10.1146/annurev-biochem-061516-044908.

Durcan, T. M. and Fon, E. A. (2015) ‘The three “ P ” s of mitophagy : PARKIN , modifications’, *Genes & development*, 29, pp. 989–999. doi: 10.1101/gad.262758.115.GENES.

Hammerling, B. C. *et al.* (2017) ‘A Rab5 endosomal pathway mediates Parkin-dependent mitochondrial clearance’, *Nature Communications*, 8. doi: 10.1038/ncomms14050.

Hsu, F. *et al.* (2018) ‘Rab5 and Alsin regulate stress-activated cytoprotective signaling on mitochondria’, *eLife*, 7, pp. 1–37. doi: 10.7554/elife.32282.

Kitamura, T. *et al.* (2003) ‘Retrovirus-mediated gene transfer and expression cloning: Powerful tools in functional genomics’, *Experimental Hematology*, 31(11), pp. 1007–1014. doi: 10.1016/S0301-472X(03)00260-1.

Klionsky, D. J. *et al.* (2016) ‘Guidelines for the use and interpretation of assays for monitoring autophagy (3rd edition)’, *Autophagy*, 12(1), pp. 1–222. doi: 10.1080/15548627.2015.1100356.

Koyano, F. *et al.* (2019) ‘Parkin recruitment to impaired mitochondria for nonselective ubiquitylation is facilitated by MITOL’, *Journal of Biological Chemistry*, 294(26), pp. 10300–10314. doi: 10.1074/jbc.RA118.006302.

Liao, W. *et al.* (2008) ‘CARP-2 Is an Endosome-Associated Ubiquitin Ligase for RIP and Regulates TNF-Induced NF-κB Activation’, *Current Biology*, 18(9), pp. 641–649. doi: 10.1016/j.cub.2008.04.017.

McDonald, E. R. and El-Deiry, W. S. (2004) ‘Suppression of caspase-8- and -10-associated RING proteins results in sensitization to death ligands and inhibition of tumor cell growth’, *Proceedings of the National Academy of Sciences of the United States of America*. National Academy of Sciences, 101(16), pp. 6170–6175. doi: 10.1073/pnas.0307459101.

McLelland, G. L. *et al.* (2016) ‘Syntaxin-17 delivers PINK1/parkin-dependent mitochondrial vesicles to the endolysosomal system’, *Journal of Cell Biology*, 214(3), pp. 275–291. doi: 10.1083/jcb.201603105.

McLelland, G. L. *et al.* (2018) ‘Mfn2 ubiquitination by PINK1/parkin gates the p97-dependent release of ER from mitochondria to drive mitophagy’, *eLife*, 7, pp. 1–35. doi: 10.7554/eLife.32866.

Montava-Garriga, L. and Ganley, I. G. (2020) ‘Outstanding Questions in Mitophagy: What We Do and Do Not Know’, *Journal of Molecular Biology*. Elsevier Ltd, 432(1), pp. 206–230. doi: 10.1016/j.jmb.2019.06.032.

Narendra, D. *et al.* (2008) ‘Parkin is recruited selectively to impaired mitochondria and promotes their autophagy’, *Journal of Cell Biology*, 183(5), pp. 795–803. doi: 10.1083/jcb.200809125.

Narendra, D. P. *et al.* (2010) ‘PINK1 is selectively stabilized on impaired mitochondria to activate Parkin’, *PLoS Biology*, 8(1). doi: 10.1371/journal.pbio.1000298.

Okiyoneda, T. *et al.* (2018) ‘Chaperone-Independent Peripheral Quality Control of CFTR by RFFL E3 Ligase’, *Developmental Cell*. Elsevier Inc., 44(6), pp. 694-708.e7. doi: 10.1016/j.devcel.2018.02.001.

Porporato, P. E. *et al.* (2018) ‘Mitochondrial metabolism and cancer’, *Cell Research*. Nature Publishing Group, 28(3), pp. 265–280. doi: 10.1038/cr.2017.155.

Puri, C. *et al.* (2018) ‘The RAB11A-Positive Compartment Is a Primary Platform for Autophagosome Assembly Mediated by WIPI2 Recognition of PI3P-RAB11A’, *Developmental Cell*. Elsevier Inc., 45(1), pp. 114-131.e8. doi: 10.1016/j.devcel.2018.03.008.

Ran, F. A. *et al.* (2013) ‘Genome engineering using the CRISPR-Cas9 system’, *Nature Protocols*, 8(11), pp. 2281–2308. doi: 10.1038/nprot.2013.143.

Santel, A. and Fuller, M. T. (2001) ‘Control of mitochondrial morphology by a human mitofusin’, *Journal of Cell Science*, 114(5), pp. 867–874.

Shaner, N. C., Patterson, G. H. and Davidson, M. W. (2007) ‘Advances in fluorescent protein technology’, *Journal of Cell Science*, 120(24), pp. 4247–4260. doi: 10.1242/jcs.005801.

Stefan, C., Audhya, A. and Emr, S. D. (2010) *FYVE domains in membrane trafficking and cell signaling*. Second Edi, *Handbook of Cell Signaling, 2/e*. Second Edi. Elsevier Inc. doi: 10.1016/B978-0-12-374145-5.00138-8.

Stewart, S. A. *et al.* (2003) ‘Lentivirus-delivered stable gene silencing by RNAi in primary cells’, *Rna*, 9(4), pp. 493–501. doi: 10.1261/rna.2192803.

Sugiura, A. *et al.* (2014) ‘A new pathway for mitochondrial quality control: mitochondrial-derived vesicles’, *The EMBO Journal*. EMBO, 33(19), pp. 2142–2156. doi:

10.15252/embj.201488104.

Tanaka, A. *et al.* (2010) ‘Proteasome and p97 mediate mitophagy and degradation of mitofusins induced by Parkin’, *Journal of Cell Biology*, 191(7), pp. 1367–1380. doi: 10.1083/jcb.201007013.

Tibbetts, M. D. *et al.* (2004) ‘Crystal structure of a FYVE-type zinc finger domain from the caspase regulator CARP2’, *Structure*, 12(12), pp. 2257–2263. doi: 10.1016/j.str.2004.10.007.

Villa, E. *et al.* (2017) ‘Parkin-Independent Mitophagy Controls Chemotherapeutic Response in Cancer Cells’, *Cell Reports*, 20(12), pp. 2846–2859. doi: 10.1016/j.celrep.2017.08.087.

Yamano, K. *et al.* (2018) ‘Endosomal rab cycles regulate parkin-mediated mitophagy’, *eLife*, 7, pp. 1–32. doi: 10.7554/eLife.31326.

Yoshii, S. R. *et al.* (2011) ‘Parkin mediates proteasome-dependent protein degradation and rupture of the outer mitochondrial membrane’, *Journal of Biological Chemistry*, 286(22), pp. 19630–19640. doi: 10.1074/jbc.M110.209338.

Figure 1

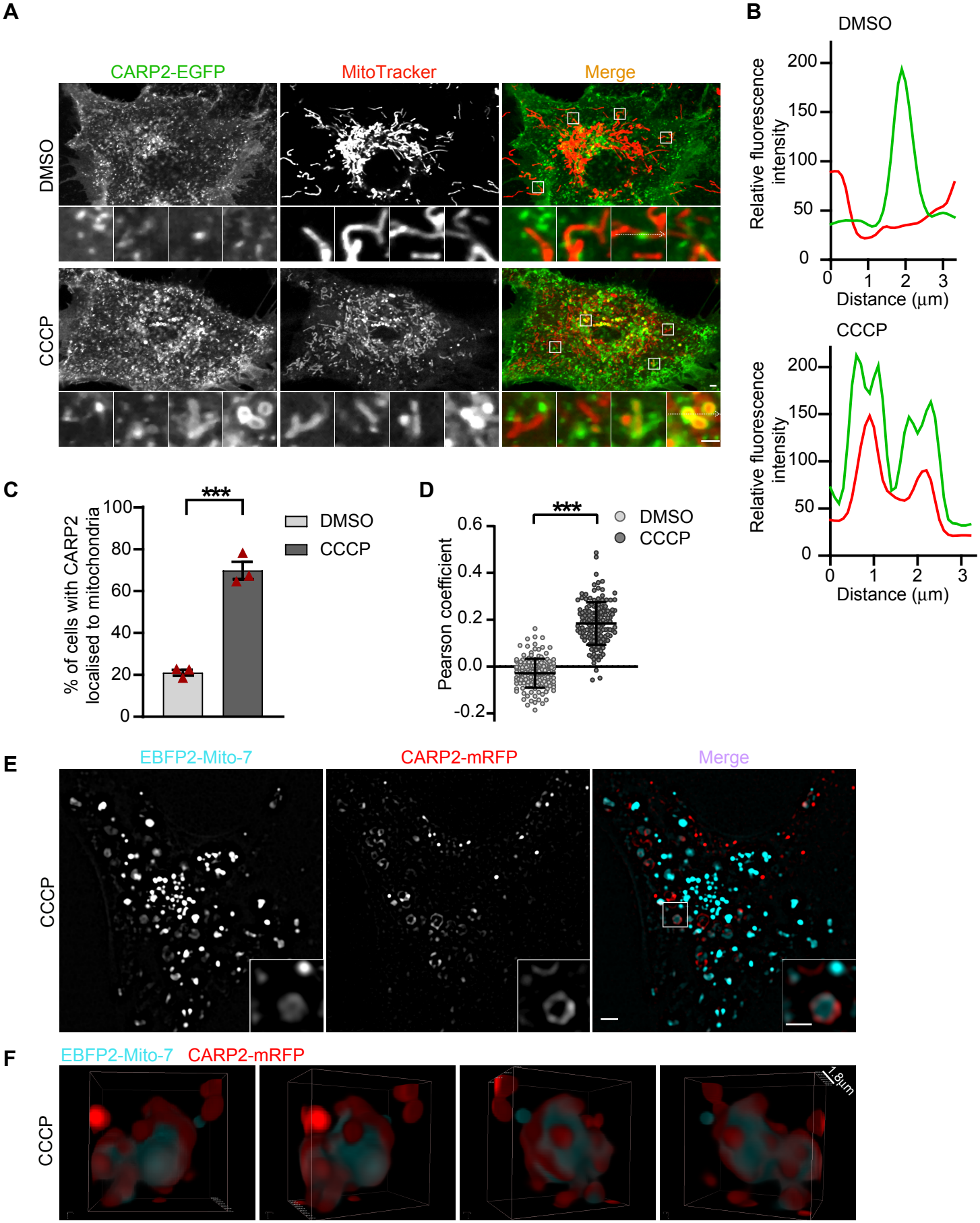
A
CARP2-EGFP
MitoTracker
Merge
DMSO
CCCP
B
DMSO
Relative fluorescence intensity
200
150
100
50
0
0
1
2
3
Distance (µm)
CCCP
Relative fluorescence intensity
200
150
100
50
0
0
1
2
3
Distance (µm)
C
***
% of cells with CARP2 localised to mitochondria
100
80
60
40
20
0
DMSO
CCCP
D
***
Pearson coefficient
0.6
0.4
0.2
0.0
-0.2
DMSO
CCCP
E
EBFP2-Mito-7
CARP2-mRFP
Merge
CCCP
F
EBFP2-Mito-7
CARP2-mRFP
CCCP
1.8µm

Figure 2

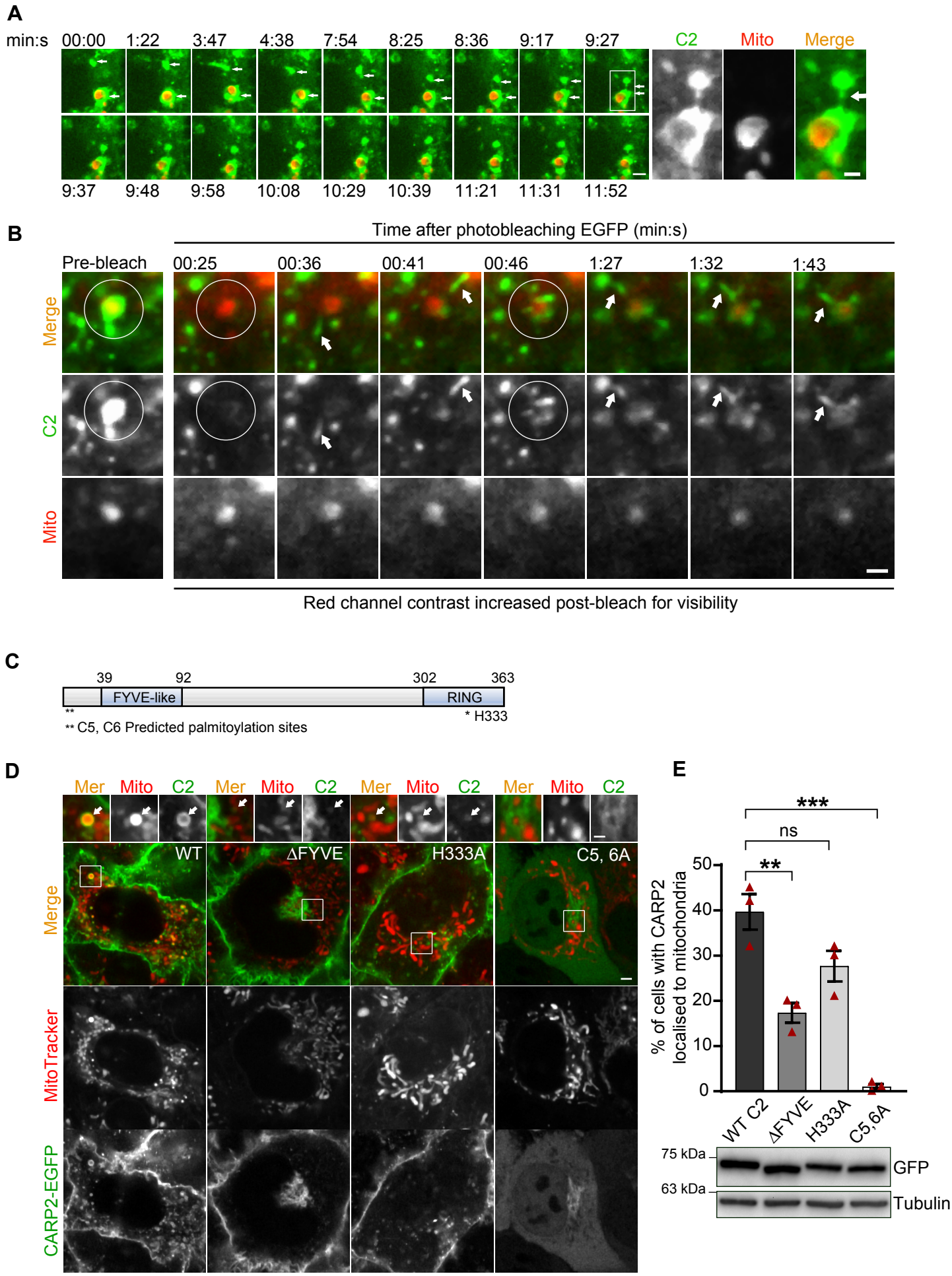
A
min:s
00:00
1:22
3:47
4:38
7:54
8:25
8:36
9:17
9:27
9:37
9:48
9:58
10:08
10:29
10:39
11:21
11:31
11:52
C2
Mito
Merge
B
Time after photobleaching EGFP (min:s)
Pre-bleach
00:25
00:36
00:41
00:46
1:27
1:32
1:43
Merge
C2
Mito
Red channel contrast increased post-bleach for visibility
C
39
92
302
363
FYVE-like
RING
**
* H333
** C5, C6 Predicted palmitoylation sites
D
Mer
Mito
C2
WT
ΔFYVE
H333A
C5, 6A
Merge
MitoTracker
CARP2-EGFP
E
***
ns
**
% of cells with CARP2 localised to mitochondria
50
40
30
20
10
0
WT C2
ΔFYVE
H333A
C5,6A
75 kDa
63 kDa
GFP
Tubulin

Figure 3

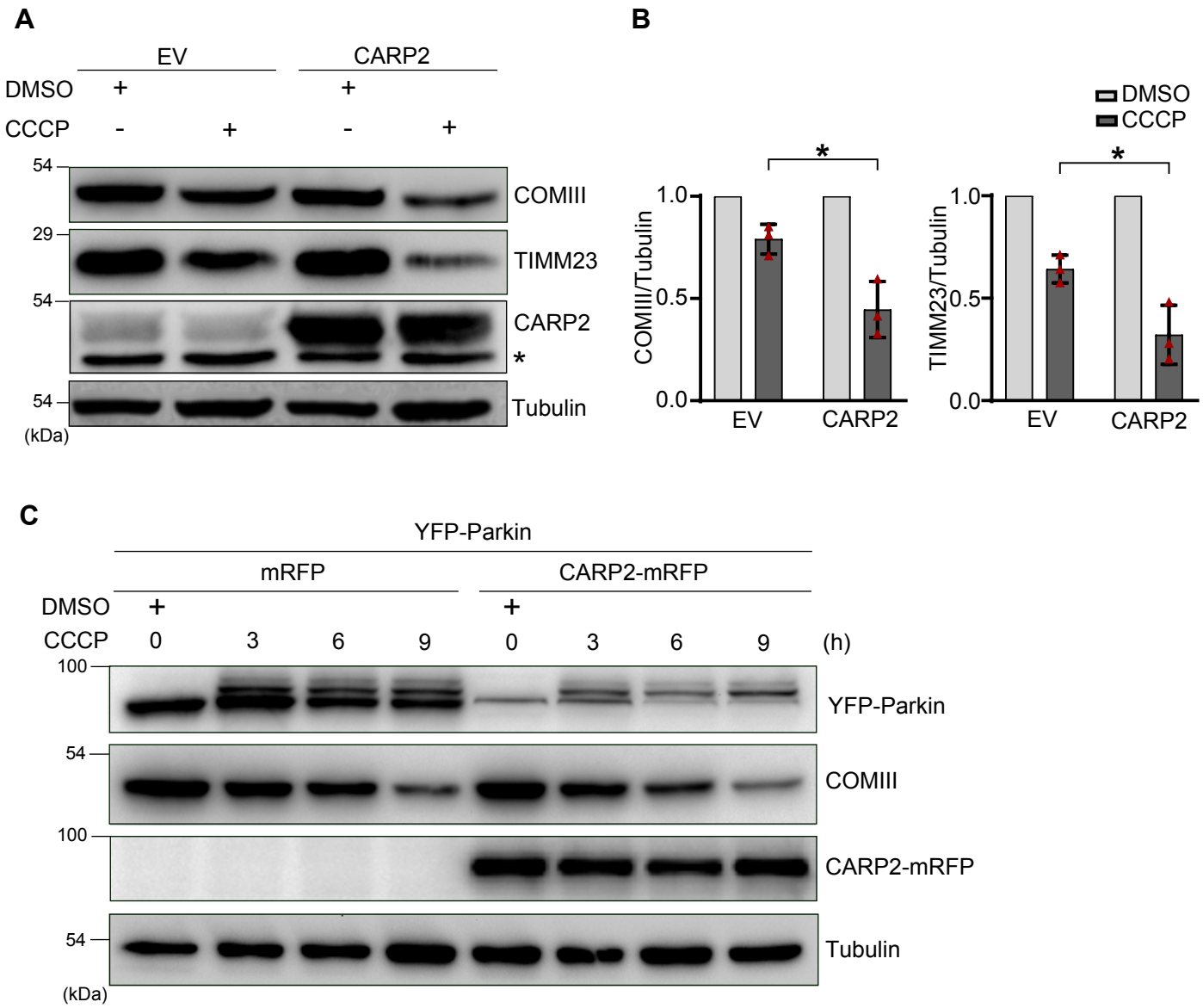
A
EV
CARP2
DMSO
CCCP
54
29
54
54
(kDa)
COMIII
TIMM23
CARP2
*
Tubulin
B
DMSO
CCCP
COMIII/Tubulin
TIMM23/Tubulin
1.0
0.5
0.0
EV
CARP2
C
YFP-Parkin
mRFP
CARP2-mRFP
DMSO
CCCP
0
3
6
9
(h)
100
54
(kDa)
YFP-Parkin
COMIII
CARP2-mRFP
Tubulin

D

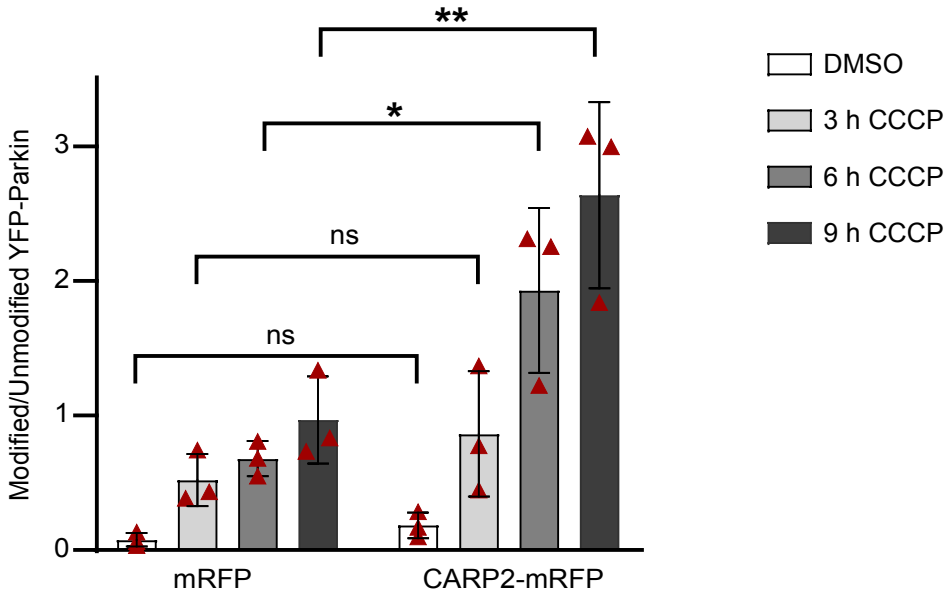
Modified/Unmodified YFP-Parkin
0
1
2
3
**
*
ns
ns
mRFP
CARP2-mRFP
DMSO
3 h CCCP
6 h CCCP
9 h CCCP

Figure 4

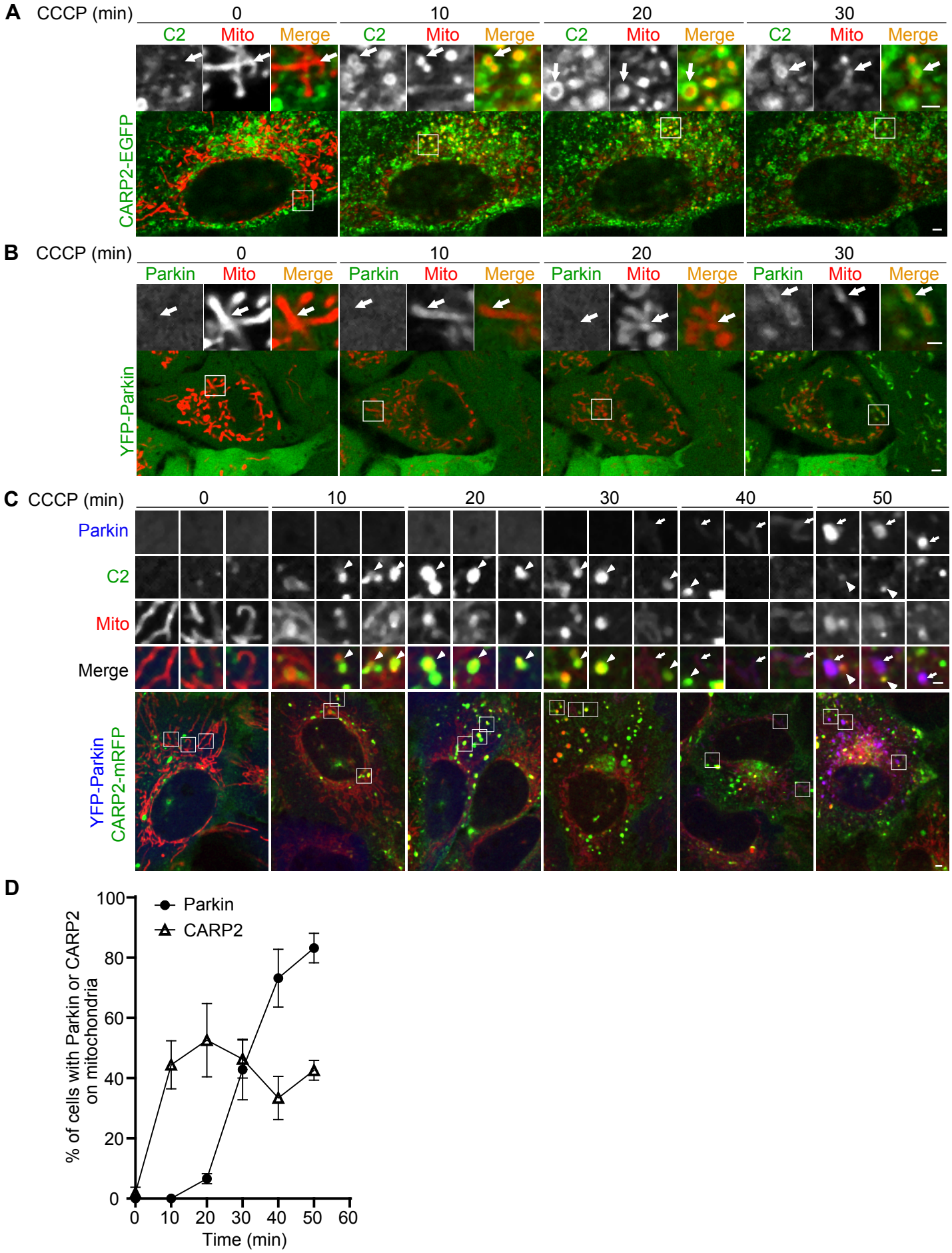
A
CCCP (min)
0
10
20
30
C2
Mito
Merge
CARP2-EGFP
B
Parkin
YFP-Parkin
C
40
50
YFP-Parkin
CARP2-mRFP
D
Parkin
CARP2
% of cells with Parkin or CARP2 on mitochondria
Time (min)
0
20
40
60
80
100

Figure 5

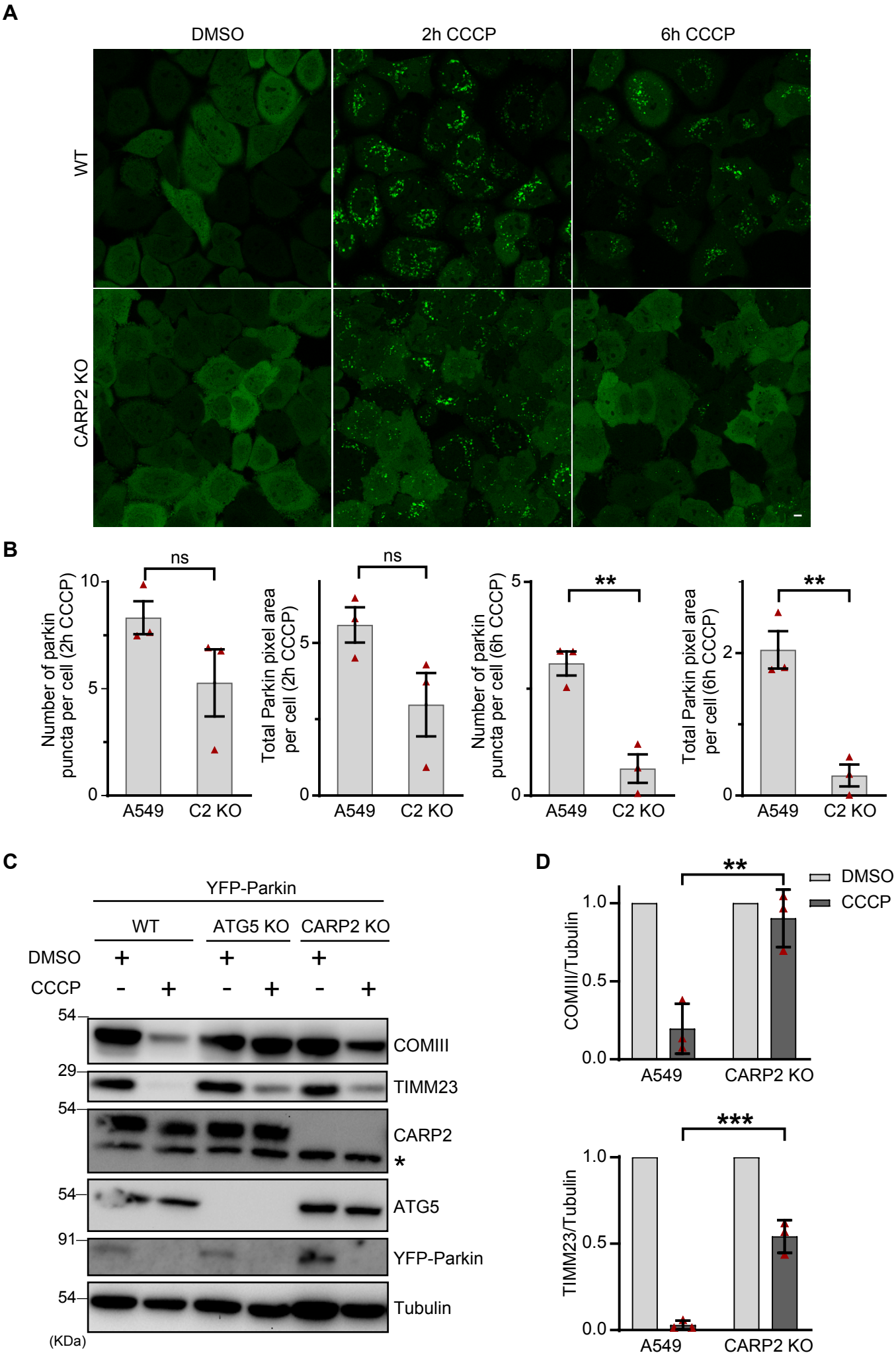
A
DMSO
2h CCCP
6h CCCP
WT
CARP2 KO
B
ns
ns
**
**
Number of parkin puncta per cell (2h CCCP)
Total Parkin pixel area per cell (2h CCCP)
Number of parkin puncta per cell (6h CCCP)
Total Parkin pixel area per cell (6h CCCP)
A549
C2 KO
C
YFP-Parkin
WT
ATG5 KO
CARP2 KO
DMSO
CCCP
COMIII
TIMM23
CARP2
*
ATG5
YFP-Parkin
Tubulin
(KDa)
D
**
***
DMSO
CCCP
COMIII/Tubulin
TIMM23/Tubulin
A549
CARP2 KO

Figure 6

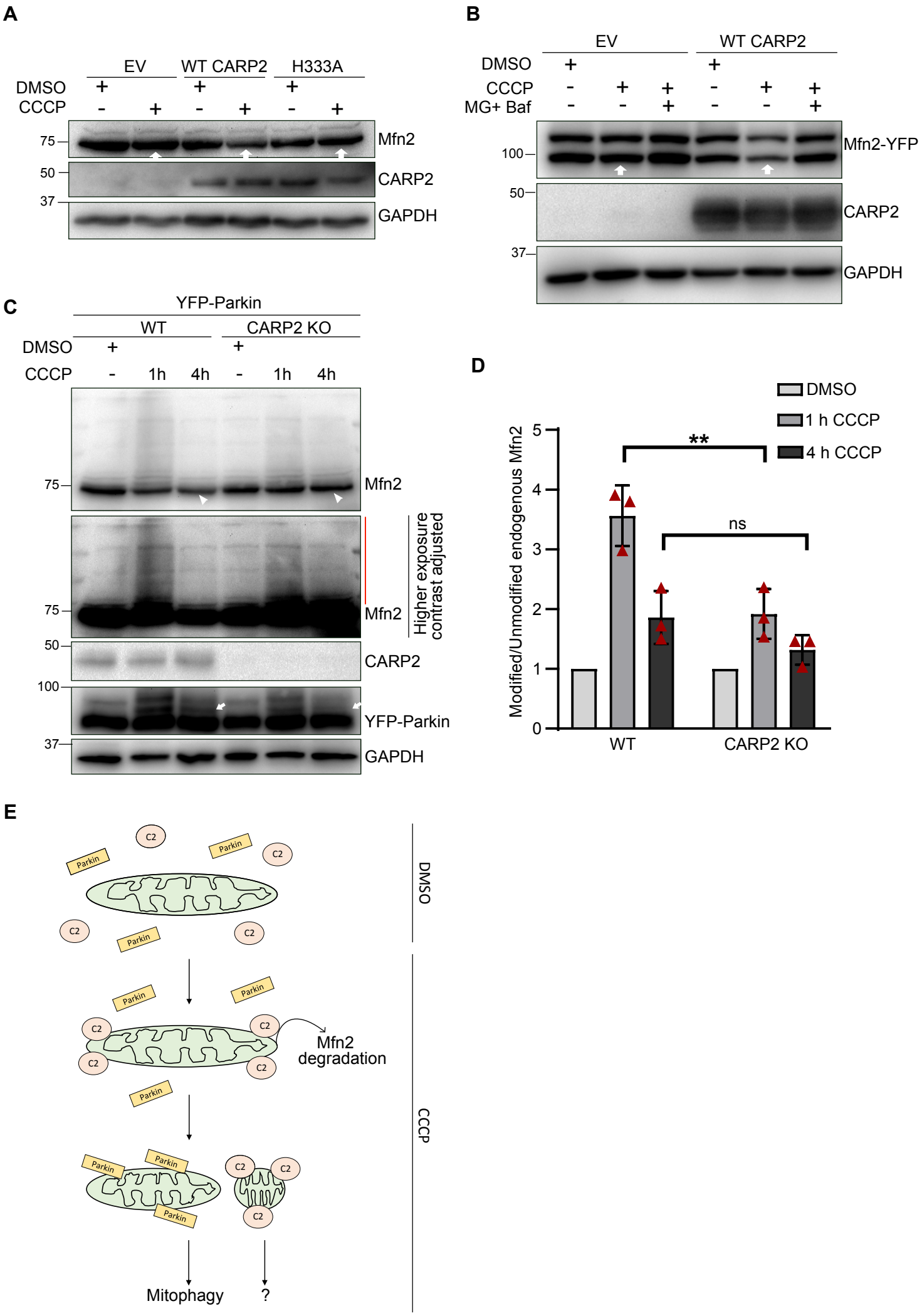
A
EV
WT CARP2
H333A
DMSO
CCCP
75
50
37
Mfn2
CARP2
GAPDH
B
EV
WT CARP2
DMSO
CCCP
MG+ Baf
100
50
37
Mfn2-YFP
CARP2
GAPDH
C
YFP-Parkin
WT
CARP2 KO
DMSO
CCCP
1h
4h
75
50
100
37
Mfn2
Higher exposure contrast adjusted
CARP2
YFP-Parkin
GAPDH
D
DMSO
1 h CCCP
4 h CCCP
Modified/Unmodified endogenous Mfn2
**
ns
WT
CARP2 KO
E
Parkin
C2
DMSO
CCCP
Mfn2 degradation
Mitophagy
?

Figure S1

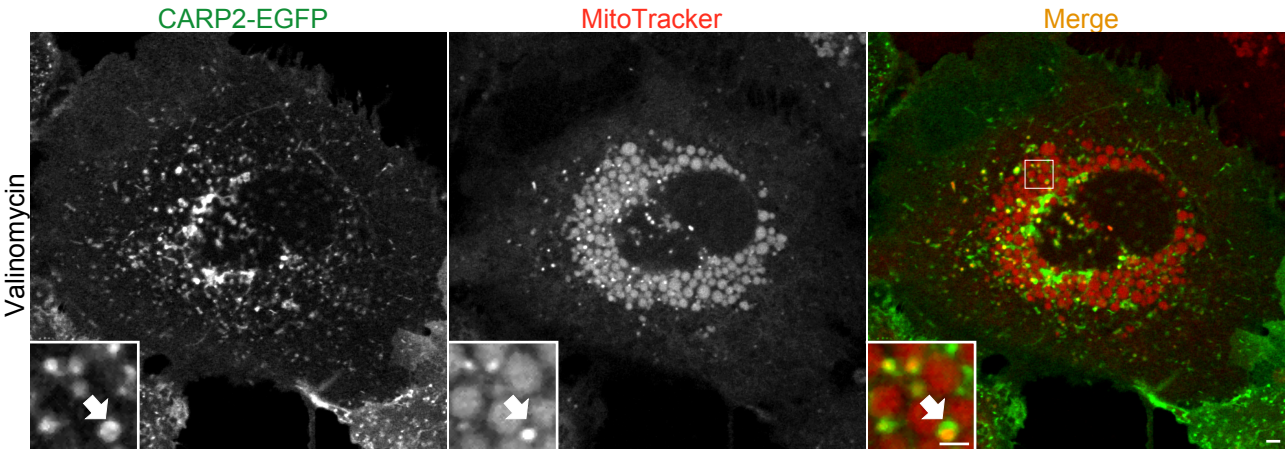

Figure S2

A

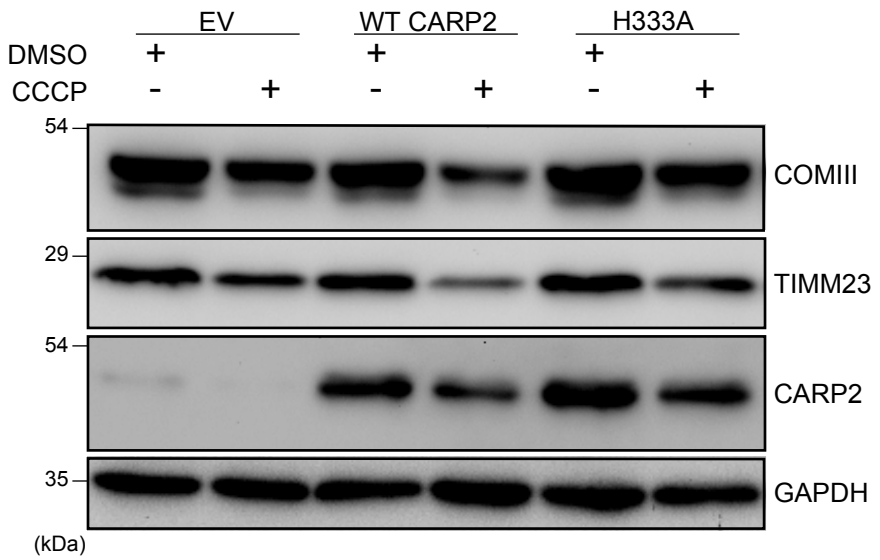
EV
WT CARP2
H333A
DMSO
CCCP
54
29
54
35
(kDa)
COMIII
TIMM23
CARP2
GAPDH

B

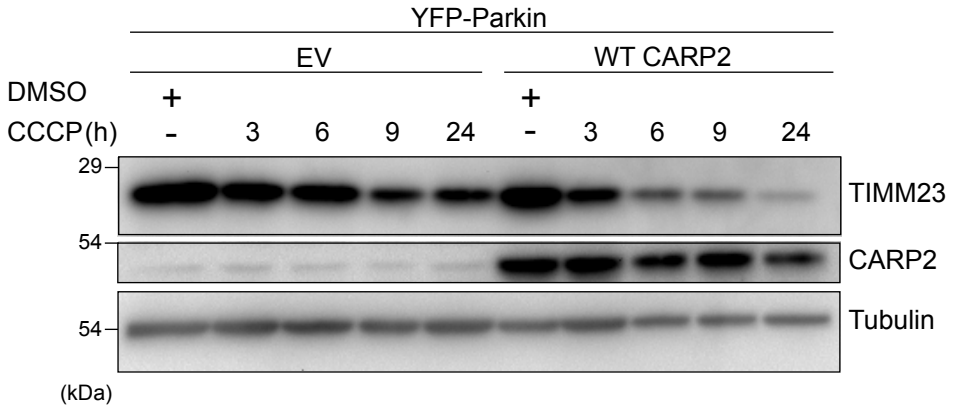
YFP-Parkin
EV
WT CARP2
DMSO
CCCP(h)
3
6
9
24
29
54
54
(kDa)
TIMM23
CARP2
Tubulin